

Trace analysis of heavy metals in groundwater samples using laser induced breakdown spectroscopy (LIBS)

WALID TAWFIK^{a,b}, LEDA G. BOUSIAKOU^{a,c,*}, RABIA QINDEEL^a, W.A.FAROOQ^a, NORAH H. ALONIZAN^a, AMAL J. FATANI^d

^aDepartment of Physics and Astronomy College of Science, King Saud University, Riyadh, Saudi Arabia.

^bDepartment of Environmental Applications NILES National Institute of Laser, Cairo University Cairo, Egypt.

^cDepartment of Automation Engineering, Piraeus University of Applied Sciences, 12241 Athens, Greece.

^dDepartment of Pharmacology, College of Science, King Saud University, Riyadh, Saudi Arabia.

This work focuses on the application of laser induced breakdown spectroscopy (LIBS) in order to detect Cr, Mn, Cu, Cd, Mg and Fe in groundwater samples from the Haier basin near Riyadh, Saudi Arabia. Considering that this is a particularly arid region, the extensively use of such groundwaters for irrigation purposes needs to be continuously monitored for elements presenting potential toxicity risks for the human health. In this method, commercial wooden sticks have been used as a substrate that absorbs the liquid sample to transform laser liquid interaction to laser solid interaction. Using the fundamental wavelength of Nd:YAG laser, the generated plasma emissions were monitored for elemental analysis. The signal-to-noise ratio SNR was optimized using laser pulse energy of 100mJ at 1064nm, while the ICDD camera detector has gate delay of 15 μ s and width of 5 μ s. In particular after samples analysis from three different wells it was found that, despite the presence of Mn, Mg and Fe, there was no detection of Cr, Cu and Cd. It is also found that the relative concentrations of the elemental content of the collected changed from one well to the other. The observed results reveal that LIBS offers a promising detection technology that not only allows the detection of a plethora of elements in the lab, but also has the potential to identify elements on site offering an immediate insight for any environmental investigation.

(Received October 24, 2014; accepted January 21, 2015)

Keywords: LIBS, Groundwater, Nd:YAG laser, Heavy metals, Toxicity

1. Introduction

Our environment and its limited natural resources are growing concerns around the world. In particular in arid regions such as Saudi Arabia, the need for water resources is paramount both as drinking water, but also for irrigation purposes. It is well known that for the latter both shallow and deep aquifer systems are used throughout the country, along with treated wastewater effluent and desalinated water. In particular such groundwater despite showing little human contamination usually tend to contain elevated levels of heavy metals or even radionuclides [1-3].

The most usual methods in analysing heavy metals in effluents is usually carried out by conventional analytic techniques such as atomic absorption spectroscopy (AAS) and UV-Vis spectrophotometry or ICMPS. Nevertheless such technologies require time-consuming sample preparation methods. Within this frame the present work aims to introduce the alternative use of laser induced breakdown spectroscopy (LIBS) that does not require such time consuming sample preparation techniques and its use in liquid samples [4, 5]. LIBS got a lot of interest in the past years, where a lot of works on LIBS in liquids ranging from small-droplets and aerosols to organic solution and molten steel have been studied [6]. In particular LIBS allows for the creation of a high-temperature plasma on

the target to be analysed. The focus of laser beams on each sample leads to the disassociation of its atoms and ions generating emission spectra that enable the detection of the elements present in the sample [7, 8]. In short, LIBS is a very useful technique to provide elemental analysis in situ without sample preparation in any state of matter, in a quasi-non-destructive way, which can be used in a wide range of environments.

LIBS measurements also consist of spectral and time-resolved analysis of the atomic and ionic emission lines generated at the surface of a sample after focusing there an intense laser pulse [6-11]. Since the early application of LIBS for diagnostic purposes, several systems have been developed for both laboratory [6-11] and field use [12], taking advantage of its unique characteristics such as quickness, no sample preparation and very low sample consumption, and excellent depth profiling [13-15].

LIBS has been used for many applications, such as observation of environmental change, characterization of geometrical, analysis of biological tissue, and analysis of fossils and works of art [6, 16-18]. Recently, LIBS has been determined under atmospheric-air pressure for line scanning, surface analysis, depth profiling, and 3D mapping of sample composition with a single instrument [19]. These advantages cause LIBS exceptionally useful technique for chemical mapping and surface analysis of bulk solid samples [19, 20].

Nevertheless, it was found that the application of LIBS in liquid sample analysis is more difficult due to surface ripples, splashing, decreasing of emitted intensity and a shorter plasma life-time [21–23]. This is mainly due to fluctuation of the laser intensities, in case of surface ripples occur, the laser focus is changed which results in variation of the generated plasma emission intensities. This is in addition to laser attenuation due to splashing that may cover the optics as well.

On the other hand, In case of LIBS of solid samples, the stability and homogeneity of the sample surface provides a uniform surface for greater sensitivity and repeatability [24-27].

In this work, wooden ice cream sticks have been used as a liquid absorber that absorbs the liquid sample contains trace elements to transform laser liquid interaction to laser solid interaction via LIBS technique. This very simple development was introduced to avoid laser liquid interaction problems to get highly sensitive measurements, good reproducibility and ease of handling. This technique can be applied in the fields of environmental pollution observing and monitoring the quality of drinking water wells.

The ability of LIBS to analyse matter independent of its physical state, allows its use in a wide range of samples. In particular if the constituents of the sample to be analysed are known, then LIBS can be used as a tool for further quantitative analysis or it could point out to the possible existence of impurities.

We have presented LIBS elemental analysis of water samples collected from shallow water aquifers at the Haier Basin, near the capital Riyadh, Saudi Arabia, focusing on the identification of hazardous heavy elements. Considering that Najd is a particularly arid region, with great need for water resources [28-30], careful studies of the ground waters being used for irrigation are required. Heavy metals pose a serious danger for our health as they can bind to structural proteins, enzymes and nucleic acid and interfere with their functioning. Long term exposure to heavy metals can have carcinogenic, central and peripheral nervous system and circulatory effects [31,32].

2. Materials and methods

The region where the samples were collected from can be seen in the map below and corresponds to groundwater wells within farmlands (Fig. 1). In total water samples from (3) wells were analysed as shown in the map below:

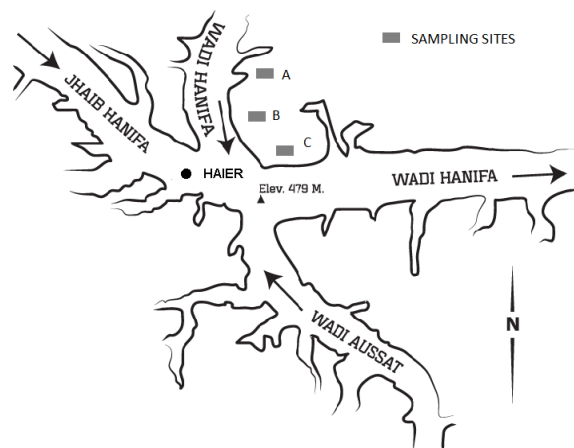


Fig. 1. The Haier Basin at the outskirts of Riyadh city, Najd and the sampling sites (wells).

Within this frame one 24-h composite water well sample was collected daily from each of the (3) wells between the months of May 2014 and July 2014; using 250ml glass for each sample they were carried using cooler boxes (to avoid degradation) to the analytical lab and were stored at 4°C according to the Standard Methods proposed by the American Public Health Association (APHA), until analysis which was conducted.

2.1 Solidification of the wastewater samples

Transformation of the liquid-phase samples (waste water) to solid phase was achieved by inserting non-contaminated, FDA approved wooden sticks of 16mm thickness, made from birch wood in 100ml of each sample and allowing them to absorb for 5 minutes each time and then left for 1 minute on dry paper. Birch wood offers a high degree of liquid absorption in a homogeneous fashion (Fig. 2). The samples were then analyzed using optimized LIBS parameters as seen in Table 1.



Fig. 2. Sample solidification before exposure to laser.

2.2 LIBS set-up and optimum parameter selection

A schematic representation of the experimental set up can be seen in Fig. 3. A Nd:YAG (Quantel, Brilliant 360mJ) was optimized to operate with pulsed energy of 100mJ at 1064nm, with pulsed width of 6ns and repetition rate of 10Hz. It was noted that at higher energy values, the dense plasma formed by the leading laser pulse start to absorb energy from the later part of the laser pulse which leads to a higher continuum emission and lower the analyte signal. Therefore at higher energies the decrease in LIBS signal might be due to shielding of laser reaching the ablation surface.

The laser beam used was then focused by a plano-convex lens of focal length 90mm to generate plasma on the surface of the specimen, which was held on a rotation motor arranged such that with every pulse there is a rotation of the sample. The laser beam reached the sample with a spot size of about a 1mm and a total of 10 shots were fired at each specimen. Additionally, the diffraction grating used was 2400 lines/mm.

Finally the light emission generated from the micro-plasma was collected using an optical fiber with 600 μm diameter, placed in the horizontal plane containing the laser beam (45° with respect to the laser beam) and fed to a high resolution spectrometer (01 nm FWHM, LOT OriEMS257) which was equipped with an ICCD camera (model DiCAM-Pro-12-Bit, PCO Computer Optics, Germany). The overall linear dispersion of the spectrometer camera system ranged between 0.006 at 200nm to 0.333 mm/pixel at 900nm. The light collection system (optical fiber) to surface distance was well controlled in order to obtain a strong spectral lines for each metal keeping the background noise at a minimum level. An energy meter (Nova 978, Ophir Optronics Ltd, USA) was used for the purpose of monitoring the shot to shot energy. The computer software used to analyze the emission lines was the Spectrum Analyser 1.7 that uses the National Institute of Standards and Technology (NIST) database.

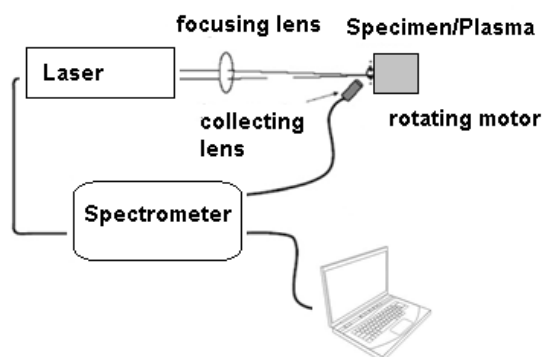


Fig. 3. Schematic representation of the LIBS system used.

The best LIBS signals were found by considering the following parameters: gain, delay, width and output as shown in Table 1.

Table 1. Parameters for Optimizing the LIBS system

Gain	Delay	Width	Output
50	15 μs	5 μs	0 μs

3. Results and discussion

3.1 Analysis of the LIBS spectrum

The typical LIBS spectrum between 350nm to 450 nm of the dry wood slices used can be seen in Fig. 3 below.

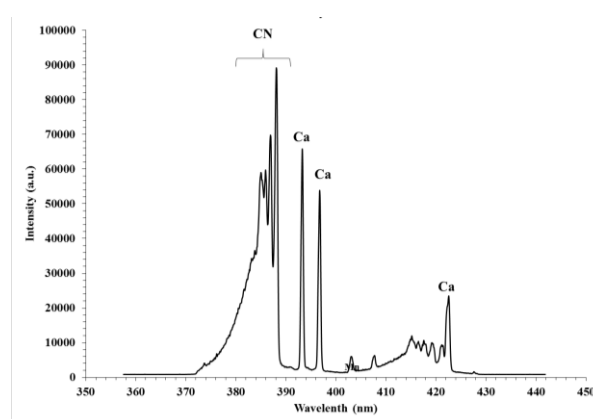


Fig. 3. The LIBS spectrum of the wood slices alone in the wavelength region of 350 nm to 450 nm before the absorption of the liquid samples.

The LIBS spectrum of the wooden slices, shows in the above region calcium (Ca), while no other contaminant such as Cr, Mn, Cu, Cd and Mg is present. Thus it is an appropriate substrate to safely proceed in checking the presence of heavy metals in our target group, identifying them in the groundwater samples. Furthermore we note the presence of CN bonds that are due to the recombination of carbon (C_2) and nitrogen (N_2) in the cooling plasma originating from the atmospheric air [33]

Additionally we note that such a direct solidification technique gives highly accurate results compared to efforts to apply LIBS to the liquid sample directly. Additionally it is a single step technique and much simpler compared to methods involving liquid to solid matrix conversion [34].

The resulting spectrum for the groundwater well (sampling site A) revealed the presence of magnesium (Mg), manganese (Mn) and iron (Fe), in the UV range while potassium (K) and sulfur (S) appear in the visible range of wavelengths (see Fig. 4). The elements Chromium (Cr), Copper (Cu) and Cadmium (Cd) are not detected within the spectrum.

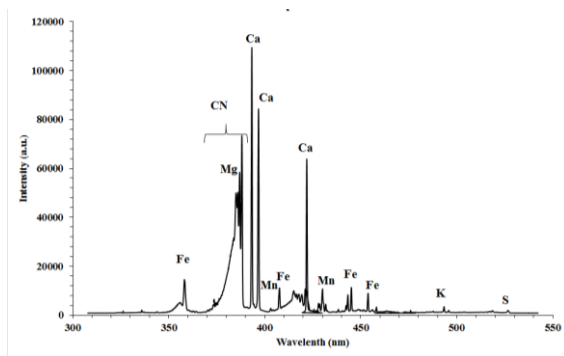


Fig. 4. The LIBS spectrum of the groundwater well (sampling site A) in the wavelength region of 350nm to 550nm.

The presence of iron (Fe) in all groundwater samples relates to the rich underground of the Saudi Arabian peninsula with Fe. In particular a number of iron (Fe) ores exist with the largest located in Wadi Sawawin, which lies in the western part of the Saudi Arabian peninsula [35]. It has been determined using software techniques that the country potentially contains over 3,000 sq. miles of iron ores, including deposits in the Najd region, where the capital Riyadh lies. Already a number of works analysing soil and agricultural products in the surrounding farmland along Wadi Hanifa, which have shown a high presence of iron [8, 35].

Furthermore in the Najd region, the main mining activities are in Al-Amar, which is a mine not only rich in gold, but also in minerals such as Mg, Mn, Cu and Zn. It is well known that water contains such macro elements in the form of ions, that are essential in sustaining biological life and Saudi water is shown to have a rich mineral profile [36-39]. Nevertheless their accumulation can prove toxic and lead to chronic poisoning.

In our analysis we detect the presence of Mg, which is essential in activating vitamin B and is involved in blood clotting [40,41]. Nevertheless in excess quantities it can lead to mental depression and cardiac arrest, thus a quantitative analysis could aid in determining its concentration limits. Similarly Mn that is essential in bone structure and metabolism can lead in increased quantities to neurotoxicity and has been found in elevated quantities in children with ADHD [42]

We note that due to the fact that minerals present in water are in ionic form they can be absorbed without difficulty by the gastrointestinal tract, thus regular quality checks of potable water sources as well as sources essential for agricultural use are essential [43]. The trace elements Chromium (Cr), Copper (Cu) and Cadmium (Cd) are not detected in that wide spectrum, using our technique.

Similarly after the absorption of the liquid samples from the sampling well B, we show again the presence of magnesium (Mg), manganese (Mn), iron (Fe) as well as traces of sodium (Na) while chromium (Cr), copper (Cu) and cadmium (Cd) are not present (Fig. 5). That should be an expected result due to the proximity of the wells

(sampling site A and B) which were at a distance of 5km apart as shown in Fig. 1. Furthermore they reconfirm the accuracy of the results displayed our sampling site A.

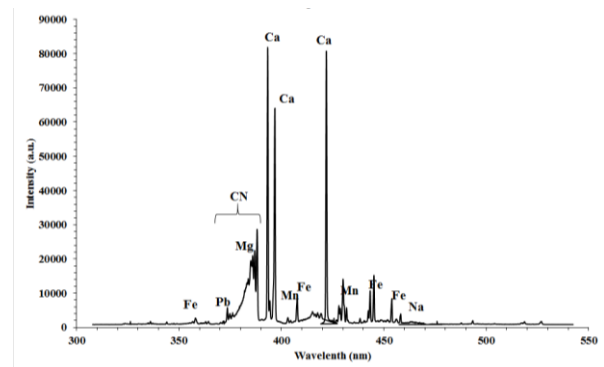


Fig. 5. The LIBS spectrum of the groundwater sample (sampling well B) in the wavelength region of 300nm to about 500 nm. None of the elements of interest appears above that wavelength range for this sample.

Finally after the absorption of the liquid samples from the sampling well C, we observe the presence of C, Mg, elements in UV range of wavelengths while iron (Fe), calcium (Ca), sodium (Na) and silicon (Si) appear in the visible range of wavelengths (Fig. 6). The elements Cr, Cu and Cd are not detected in that wide spectrum as well.

Considering again the proximity of the sampling sites-sampling site C was 3km from sampling site B, we have a consistent assessment of mineral elements that appear in all (3) sites showing that our LIBS analysis exhibits the required accuracy.

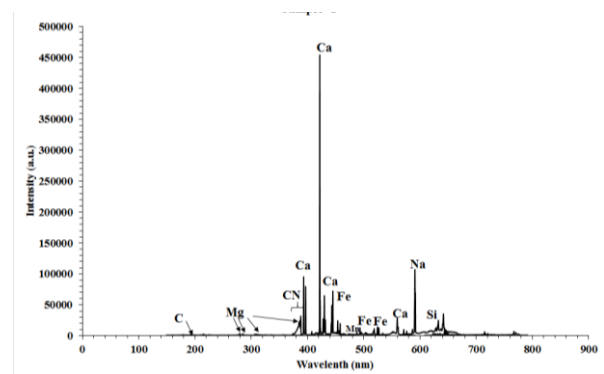


Fig. 6. The LIBS spectrum of the groundwater sample (sampling well C) in the wavelength region of 300nm to 800nm.

3.2 The emission lines present in the elements detected

Each emission line was confirmed using the National Institute of Standards and Technology (NIST) electronic database [44]. In Table 2 below, we can see the list of transitions present in the groundwater trace elements in all (3) sampling sites.

Table 2. The spectroscopic data for the resolved spectral lines of well water samples for the range from 200 nm – 800 nm.

Element wavelength (nm)	A_{ki} (S^{-1})	E_i (cm^{-1})	E_k (cm^{-1})	Configurations	g_k
Fe I 357.2	2.89E+07	22 845.869	50 833.438	$3d^6(^5D)4s4p(^3P^o) - 3d^6(^5D)4s(^6D)4d$	11
Fe I 368.6	3.34E+07	23 711.456	50 833.438	$3d^6(^5D)4s4p(^3P^o) - 3d^6(^5D)4s(^6D)4d$	11
Fe I 406.359	6.65E+07	12 560.934	37 162.746	$3d^7(^4F)4s - 3d^7(^4F)4p$	7
Fe I 440.475	2.75E+07	12 560.934	35 257.324	$3d^7(^4F)4s - 3d^7(^4F)4p$	9
Fe I 441.512	1.19E+07	12 968.554	35 611.625	$3d^7(^4F)4s - 3d^7(^4F)4p$	7
Fe II 453.416	2.30E+07	23 031.300	45 079.879	$3d^6(^3F^2)4s - 3d^6(^5D)4p$	6
Fe I 455.445	4.70E+07	23 110.939	45 061.329	$3d^6(^5D)4s4p(^3P^o) - 3d^6(^5D)4s(^6D)5s$	7
Fe I 492.05	3.58E+07	22 845.869	22 845.869	$3d^6(^5D)4s4p(^3P^o) - 3d^6(^5D)4s(^6D)5s$	9
Fe I 495.76	4.22E+07	22 650.416	42 815.855	$3d^6(^5D)4s4p(^3P^o) - 3d^6(^5D)4s(^6D)5s$	11
Fe I 520.859	6.23E+06	26 140.179	45 333.875	$3d^6(^5D)4s4p(^3P^o) - 3d^6(^5D)4s(^6D)5s$	5
Fe I 526.953	1.27E+06	6 928.268	25 899.989	$3d^7(^4F)4s - 3d^6(^5D)4s4p(^3P^o)$	9
Fe I 532.804	1.15E+07	7 376.764	26 140.179	$3d^7(^4F)4s - 3d^6(^5D)4s4p(^3P^o)$	7
Fe I 537.149	1.05E+07	7 728.060	26 339.696	$3d^7(^4F)4s - 3d^6(^5D)4s4p(^3P^o)$	5
Fe I 540.577	1.09E+07	7 985.785	26 479.381	$3d^7(^4F)4s - 3d^6(^5D)4s4p(^3P^o)$	3
Fe I 558.676	2.19E+07	27 166.820	45 061.329	$3d^6(^5D)4s4p(^3P^o) - 3d^6(^5D)4s(^6D)5s$	7
Si I 634.710	5.84e+07	65 500.47	81 251.32	$3s^2 4s^2 3s_{1/2} - 3s^2 4p(^2P^o)_{3/2}$	4
Si I 637.136	6.84e+07	65 500.47	81 191.34	$3s^2 4s^2 3s_{1/2} - 3s^2 4p(^2P^o)_{1/2}$	2
Mg II 279.07	4.01E+08	35 669.31	71 491.06	$2p^6 3p - 2p^6 3d$	4
Mg II 279.552	2.60E+08	0	35 760.88	$2p^6 3s - 2p^6 3p$	4
Mg II 279.79	7.98E+07	35 760.88	71 491.06	$2p^6 3p - 2p^6 3d$	4
Mg II 280.27	2.57E+08	0	35 669.31	$2p^6 3s - 2p^6 3p$	2
Mg I 285.212	4.91E+08	0	35 051.264	$2p^6 3s^2 - 3s 3p$	3
Mg I 383.829	1.61E+08	21 911.178	47 957.045	$3s 3p - 3s 3d$	7
Mg I 516.732	1.13E+07	21 850.405	41 197.403	$3s 3p - 3s 4s$	3
Mg I 517.268	3.37E+07	21 870.464	41 197.403	$3s 3p - 3s 4s$	3
Mg I 518.36	5.61E+07	21 911.178	41 197.403	$3s 3p - 3s 4s$	3
Ca II 393.366	1.47E+08	0	25 414.40	$3p^6 4s - 3p^6 4p$	4
Ca II 396.847	1.40E+08	0	25 191.51	$3p^6 4s - 3p^6 4p$	2
Ca 422.673	2.18E+08	0	23 652.304	$3p^6 4s^2 - 3p^6 4s 4p$	3
Ca I 428.301	4.34E+08	15 210.063	38 551.558	$3p^6 4s 4p - 3p^6 4p^2$	5
Ca I 428.936	6.00E+07	15 157.901	38 464.808	$3p^6 4s 4p - 3p^6 4p^2$	3
Ca I 430.252	1.36E+08	15 315.943	38 551.558	$3p^6 4s 4p - 3p^6 4p^2$	5
Ca I 443.495	6.70E+07	15 210.063	37 751.867	$3p^6 4s 4p - 3p^6 4s 4d$	5
Ca I 445.477	8.70E+07	15 315.943	37 757.449	$3p^6 4s 4p - 3p^6 4s 4d$	7
Ca I 559.446	3.80E+07	20 349.260	38 219.118	$3p^6 3d 4s - 3p^6 3d 4p$	5
Ca I 559.848	4.30E+07	20 335.360	38 192.392	$3p^6 3d 4s - 3p^6 3d 4p$	3
Ca I 643.907	5.30E+07	20 371.000	35 896.889	$3p^6 3d 4s - 3p^6 3d 4p$	9
Ca I 646.256	4.70E+07	20 349.260	35 818.713	$3p^6 3d 4s - 3p^6 3d 4p$	7
Ca I 649.378	4.40E+07	20 335.360	35 730.454	$3p^6 3d 4s - 3p^6 3d 4p$	5
Na I 568.263	1.01E+04	16956.1705	34 548.764	$2p^6 3p - 2p^6 4d$	4
Na I 568.820	1.21E+07	16973.3669	34 548.729	$2p^6 3p - 2p^6 4d$	6
Na I 588.994	6.16E+07	0	16973.366	$2p^6 3s - 2p^6 3p$	4
Na I 589.592	6.14E+07	0	16956.170	$2p^6 3s - 2p^6 3p$	2
Mn I 403.079	1.70E+07	0	24802.25	$3d^5 4s^2 - 3d^5(6S)4s 4p(^3P^o)$	8
Mn I 403.306	1.58E+07	0	24779.32	$3d^5 4s^2 - 3d^5(6S)4s 4p(^3P^o)$	4
Mn I 475.404	3.03e+07	18 402.46	39 431.31	$3d^5(^6S)4s 4p(^3P^o) - 3d^5 4s(^7S)5s$	8
Mn I 482.352	4.99e+07	18 705.37	39 431.31	$3d^5(^6S)4s 4p(^3P^o) - 3d^5 4s(^7S)5s$	8
K I 404.4136	1.16e+06	0	24 720.139	$3p^6 4s^2 3s_{1/2} - 3p^6 4p^2 P^o$	4
K I 766.491	3.80E+07	0	13042.896	$3p^6 4s - 3p^6 4p$	4
K I 769.897	3.75E+07	0	12985.185	$3p^6 4s - 3p^6 4p$	2
CN Swan Violet system ($B^2\Sigma^+ - X^2\Sigma^+$) From 384 – 388 nm					

3.3. A comparison in the intensities of the elements between the sampling sites

In a particular matrix, intensity of an elemental line in LIBS spectra is always proportional to quantity of the element present in a sample in other words we can calculate abundance ratio of the constituents of the sample using corresponding highest line intensities [8, 45].

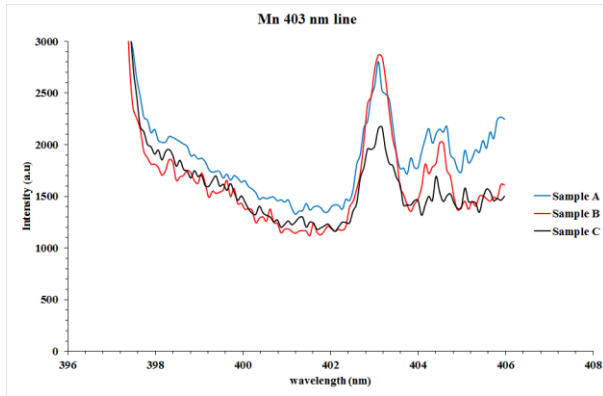


Fig. 7. Comparison of Mn line at 403 nm for three samples.

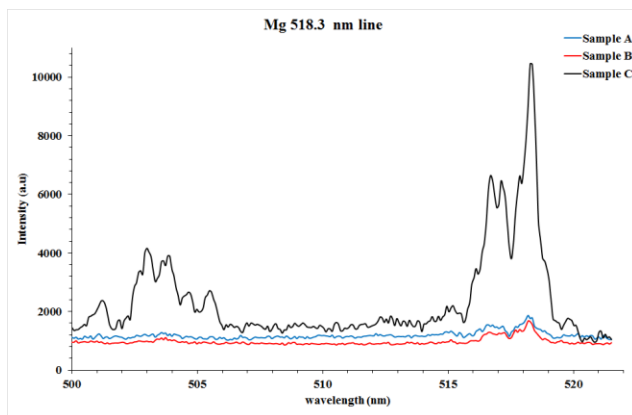


Fig. 8. Comparison of Mg line at 518.3 nm for three samples.

Comparison of abundance of Mn, Mg, Fe and Ca can be estimated in the samples from Figs. 7, 8, 9 and 10 respectively. Fig. 7 shows that quantity of Mn in sample-A and sample-B is almost equal but it is almost half in sample-C as compared to the Mn quantities of sample-A & sample-B. Similarly Fig. 8 shows that quantity of Mg is highest in sample-C and very little in sample-A & B. Quantities of Fe and Ca are highest in sample-A which can be seen in Figs. 9 & 10. Fig. 10 reveals that there is little difference in quantity of Ca in the samples A, B & C.

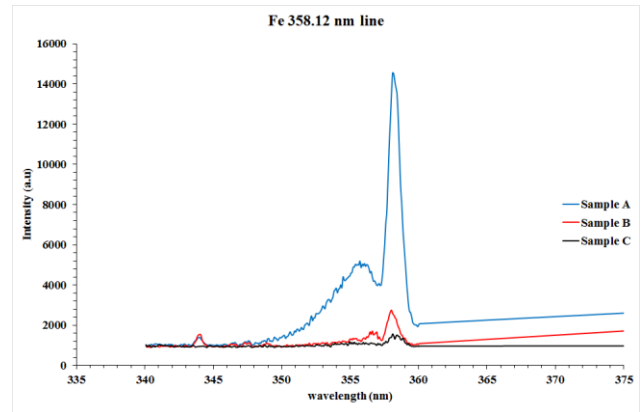


Fig. 9. Comparison of Fe line at 358.12 nm for three samples.

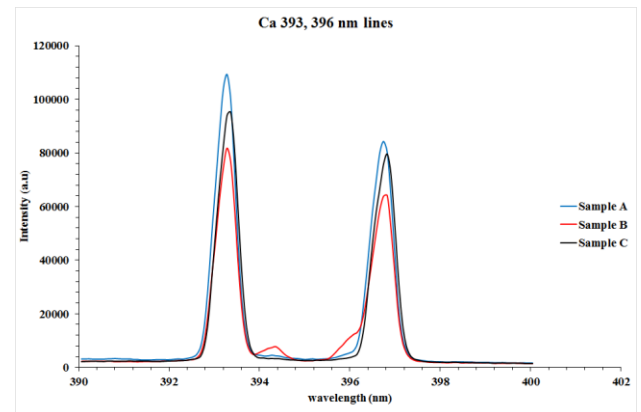


Fig. 10. Comparison of Ca line at 393 & 396 nm for three samples.

4. Conclusions

We have presented traces of heavy elements in groundwater samples from the Haier Basin near Riyadh using LIBS. In particular by transforming laser liquid interaction to laser solid interaction we have managed to show the presence of Mn, Mg and Fe, while there was no detection of Cr, Cu and Cd. Our method used the fundamental wavelength of Nd:YAG laser and the signal-to-noise ratio SNR was optimized using laser pulse energy of 100mJ at 1064nm, while the ICDD camera detector has gate delay of 15 μ s and width of 5 μ s. Additionally a comparison of abundance of Mn, Mg, Fe and Ca was estimated from all (3) groundwater wells. The observed results show that LIBS not only allows the detection of elements in the lab, but also can provide a reliable tool for onsite identification of a plethora of elements in any environmental investigation.

Acknowledgements

This project was supported by King Saud University, Deanship of Scientific Research, College of Science Research Centre.

The authors would like to thank Mr. Amjad Mazhar, senior technician at the Department of Physics and Astronomy, King Saud University.

References

- [1] John DeZuane "Handbook of Drinking Water Quality" Wiley; 2 edition (December 31, 1996).
- [2] Mahbub Hussaina, Syed Munaf Ahmedb, Walid Abderrahmanc, Journal of Environmental Management, **88**, 297 (2008).
- [3] ASTM "Annual book of ASTM standards 11.02" Philadelphia, PA, American Society for Testing and Materials (1994).
- [4] A. W. Miziolek, V. Palleschi, I. Schechter, Cambridge University Press, (2006) ISBN 978-0-521-85274-6.
- [5] B. Charfi, M. A. Harith, Spectrochimica Acta Part B: Atomic Spectroscopy, **57**(7), 1141 (2002).
- [6] J. P. Singh, S. N. Thakur, Elsevier Science, (2007).
- [7] W. A. Farooq, F. N. Al-Mutairi, Z. Alahmed, Optics and Spectroscopy, **115**(2), 241 (2013).
- [8] W. A. Farooq, F. N. Al-Mutairi, A. E. M. Khater, A. S. Al-Dwayyan, M. S. AlSalhi, M. Atif, Optics and Spectroscopy, **112**(6), 874 (2012).
- [9] W. A. Farooq, W. Tawfik, Z. A. Alahmed, K. Ahmad, J. P. Singh, Journal of Russian Laser Research, **35**(3), May, 2014.
- [10] M. Casini, M. A. Harith, V. Palleschi, A. Salvetti, D. P. Singh, M. Vaselli, Laser and Particle Beams, **9**(2), 633 (1991).
- [11] Meirong Dong, Xianglei Mao, Jhanis J. Gonzalez, Jidong Lu, Richard E. Russo, Anal. At. Spectrom., **27**, 2066 (2012).
- [12] C. M. Davies, H. H. Telle, D. J. Montgomery, R. E. Corbett, Spectrochimica Acta Part B: Atomic Spectroscopy, **50**(9), 1059 (1995).
- [13] M. Darby Dyar, Jonathan M. Tucker, Seth Humphries, Samuel M. Clegg, Roger C. Wiens, Melissa D. Lane, Spectrochimica Acta Part B: Atomic Spectroscopy, **66**(1), 39 (2011).
- [14] Jer-Shing Huang, Hsiao-Tsui Liu, King-Chuen Lin, Analytica Chimica Acta **581**, 303 (2007).
- [15] F. Anabitarte, A. Cobo, J. M. Lopez-Higuera, International Scholarly Research Network ISRN Spectroscopy, 2012, Article ID 285240, 12 pages doi:10.5402/2012/285240.
- [16] D. A. Cremers, L. J. Radziemski, J. Wiley, Handbook of Laser-Induced Breakdown Spectroscopy, John Wiley & Sons, 2006.
- [17] J. Diedrich, S. J. Rehse, S. Palchaudhuri Appl. Phys. Lett. **90**, 163901-1~163901-3 (2007).
- [18] A. C. Samuels, F. C. DeLucia Jr., K. L. McNesby, A. W. Miziolek, Appl. Opt. **42**, 6205 (2003).
- [19] M. Banaee, S. H. Tavassoli, Polymer Testing **31**, 759 (2012).
- [20] Walid Tawfik, W. Aslam Farooq, Z. A. Alahmed, J. Opt. Soc. Korea **18**(1), 50 (2014).
- [21] D. R. Anderson, C. W. McLeod, T. English, A. T. Smith, Appl. Spectrosc. **49**, 691 (1995).
- [22] Walid Tawfik Y. Mohamed, International Journal of Pure and Applied Physics, **2**(1), 11 (2006).
- [23] M. Soliman, W. Tawfik, M. A. Harith, Cairo, Egypt, Forschungszentrum Juelich GmbH, Bilateral Seminars of the International Bureau, **34**, 240 (2003).
- [24] B. Charfi, M. A. Harith, Spectrochim. Acta Part B, **57**, 1141 (2002).
- [25] W. A. Farooq, Walid Tawfik, A. Fatehmulla, S. M. Ali, M. Aslam IEEEExplore, CAOL*2013 International Conference on Advanced Optoelectronics & Lasers, 09-13 September, (2013), Sudak, Ukraine.
- [26] Walid Tawfik, W. Aslam Farooq, Zeyad A. Alahmed, M. Sarfraz, Fahrettin Yakuphanoglu, IEEEExplore, Electronics, Communications and Photonics Conference (SIEPC), 2013 Saudi International.
- [27] D. E. Lencioni, Appl Phys Lett. **25**(1), 15 (1974).
- [28] Mohammed J. Abdulrazzak, Groundwater system evaluation for Wadi Nisah, Saudi Arabia, Msc Thesis, University of Arizona (1976).
- [29] Leda G. Bousiakou, M. Kazi, P. Lianos, Amal J. Fatani, E. Kalkani, George Karikas, Pharmakeytiki Journal **25** (I) 2013.
- [30] Abdullah A. Alibrahim, Ambio, **20**(1), (1991).
- [31] W. G. Landis, R. M. Sofield, M.-H. Yu, Introduction to Environmental Toxicology: Molecular Substructures to Ecological Landscapes, 4th ed., CRC Press, Boca Raton, Florida, ISBN 9781439804100, 2000, P.269 OLD 28-NEW 29.
- [32] M. W. F. Nielen, H. J. P. Marvin, in Y Picó (ed.), Food Contaminants and Residue Analysis, Comprehensive Analytical Chemistry, **51**, Elsevier, Amsterdam, ISBN 0080931928, 2008, pp. 1–28.
- [33] Matthieu Baudelet, Laurent Guyon, Jin Yu, Jean-Pierre Wolf, Tanguy Amodeo, Emeric Fréjafon, Patrick Laloi, Appl. Phys. Lett. **88**, 063901 (2006).
- [34] D. M. Díaz Pace, C. A. D'Angelo, D. Bertuccelli, G. Bertuccelli, Spectrochimica Acta Part B: Atomic Spectroscopy, **61**(8), 929 (2006).
- [35] <http://www.londonmining.com/operations/saudi-arabia>
- [36] A. Aly, A. Alomran, M. Alwabel, A. Almahaini, Mohammed Alamari, Proceedings of the International Academy of Ecology and Environmental Sciences, **3**(1), 42 (2013).
- [37] Z. A. Tayyeb, S. M. Farid, K. A. Otaibi, Journal of King Abdul Aziz University: Engineering Science, **15**, 149 (2004).
- [38] I. Al-Saleh, I. Al-Doush, Science of the Total Environment, **216**, 181 (1998).
- [39] S. M. Alfadul, M. A. Khan, Journal of Environmental Science and Health, Part A. Toxic/Hazardous Substances and Environmental Engineering, **46**, 1519 (2011).
- [30] WHO (World Health Organisation) Significance of calcium and magnesium in drinking water, Public Health significance (2009) pp 18.

- [31] F. Kozisek, Health significance of drinking water calcium and magnesium. (2003), <http://www.szu.cz/chzp/voda/pdf/hardness.pdf>
- [32] A. C. Farias, J Child Adolesc Psychopharmacol 2010, **20**(2):113-8. doi: 10.1089/cap.2009.0073.
- [33] WHO (World Health Organization), Guidelines for drinking water quality.4th ed.; WHO Press: World Health Organization, 20 Avenue Appia, 1211 Geneva 27, Switzerland, 2011, 1-518.
- [34] NIST electronic database, <http://physics.nist.gov/PhysRefData/contents-atomic.html>.
- [35] S. Mahmood, S. A. Abbasi, S. Jabeen, M. A. Baig, Journal of Quantitative Spectroscopy & Radiative Transfer **111**, 689 (2010).

*Corresponding author: leda07@hotmail.com